Conformation Analysis

Carbopeptoid Folding: Effects of Stereochemistry, Chain Length, and Solvent**

*Riccardo Baron, Dirk Bakowies, and Wilfred F. van Gunsteren**

The folding of a polypeptide chain into the stable three-dimensional structure of a biologically active protein is still not understood in atomic detail. However, several research groups have recently reported successful atomistic simulations of secondary-structure formation, including the formation of helices of different types, β turns and β sheets of α- and β-peptides.[1–23] Insight into the nature of both the folding process[24,25] and the unfolded state[15,26,27] has been obtained from various studies simulating the reversible folding of peptides. This development is encouraging and indicates that the biomolecular force fields in use are approaching the accuracy required to predict folding equilibria, although this has so far been demonstrated only for short polypeptides.

Experimentally, significant progress has been made in the design and synthesis of peptide analogues that mimic secondary-structure elements of proteins, such as α helices, turns, and β sheets.[28–30] For example, carbopeptoids, homo-oligomers of sugar-containing amino acids, have been prepared with both furanose[31] and pyranose[32] residues. These carbopeptoids are members of the family of δ-peptides which may formally be constructed from α-peptides by replacement of every second peptide fragment with a substituted tetrahydrofuran (THF) or tetrahydropyran ring.[33] These molecules have potential applications as drugs that block protein–protein interactions and inhibit enzyme catalysis.[34–36]

Structural preferences have been investigated in nuclear magnetic resonance (NMR) experiments.[31,37–40] Various oligomers with *cis* configurations at the C2 and C5 atoms of the THF ring (Scheme 1) tend to form conformations reminiscent of a conventional β turn.[41] The characteristic NH(i)–O(i–2) hydrogen-bonding pattern has been observed for tetramer **1** in both chloroform and dimethylsulfoxide (DMSO).[37] Chain extension to six or eight residues does not alter the preferred secondary structure. Apparently, hexamer **2** and octamer **3** show the hydrogen-bonding pattern of tetramer **1**, extended to six and eight residues, respectively. The *trans*-linked tetramers appear to have no conformational

[*] R. Baron, Dr. D. Bakowies, Prof. Dr. W. F. van Gunsteren
Laboratorium für Physikalische Chemie, ETH Zürich
8093 Zürich (Switzerland)
Fax: (+41) 1-632-1039
E-mail: wfvgn@igc.phys.chem.ethz.ch

[**] Financial support from the Schweizerischer Nationalfonds (Project no.: 2000-063590) and from the National Center of Competence in Research (NCCR), Structural Biology, of the Swiss National Science Foundation (SNSF) is gratefully acknowledged. We thank Dr. Tim Claridge for providing us with NMR spectroscopic data for the *cis*-tetramer **1**.

Supporting information for this article is available on the WWW under http://www.angewandte.org or from the author.

 DOI: 10.1002/ange.200454114

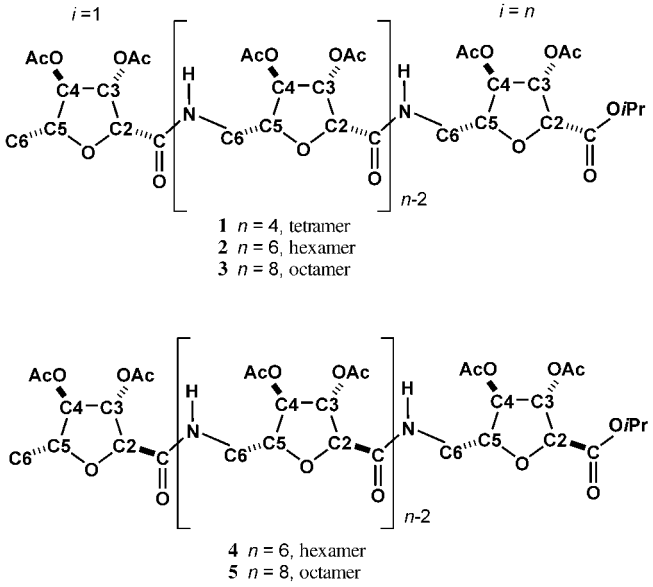

Scheme 1. Chemical formulas of the peptides studied. The numbering referred to in the text is indicated.

preferences or to adopt other types of structure, depending on the substituents at the C3 and C4 positions.[31] The *trans* octamer **5** with ketal protecting groups at the C3 and C4 positions is reported to form a rare type of left-handed helix, stabilized by interresidue NH(*i*)–O(*i*–3) hydrogen bonds.[31,40]

The apparent dependence of structural motifs on chain length and stereochemistry prompted us to carry out molecular dynamics (MD) simulations to supplement the indirect experimental observations with a more detailed atomistic picture. Scheme 1 shows the peptides considered in the present study. Tetramer **1**, hexamer **2**, and octamer **3** are all based upon a *cis*-linked β-D-*arabino*-furanose scaffold. Hexamer **4** and octamer **5** are the corresponding *trans*-linked stereoisomers. All simulations were performed with chloroform as solvent. An additional simulation of tetramer **1** in DMSO was performed to assess the effect of solvent on secondary-structure formation.

The accuracy of MD simulations may be assessed by comparison to results from nuclear Overhauser effect (NOE) experiments. Qualitative NOE intensities have been reported for tetramer **1** in chloroform.[37] Table 1 lists these data and compares them with $\langle r^{-3}\rangle^{-1/3}$ averages of proton–proton r distances computed from the MD trajectory and with the corresponding distances of a structure modeled to satisfy all NOE distance limits. Generally, proton pairs showing an NOE signal are expected to have an average distance of 0.5 nm or less, and strong signals indicate shorter distances. Inspection of Table 1 shows that the MD simulation satisfies all experimentally derived distance limits, except those for N(4)–C3(2), N(3)–C3(1), and C6(3)-*pro*-S–C3(1). However, all of these three proton pairs show weak signals experimentally. The distance analysis has also been performed separately for the three most populated clusters of structures, subsets of the MD trajectory that contain only structures that are very similar to each other. Clusters 1 and 3 show N(3)–C3(1) and N(4)–C3(2) proton-pair distances, respectively, which are within experimental limits. Likewise, the average distance of the proton pair C6(3)-*pro-S*–C3(1) is noticeably smaller for cluster 1 than it is for the entire trajectory. These observations indicate that all experimentally derived proton–proton contacts are reproduced by the MD simulation, although the distribution of distances for three proton–proton pairs may be inaccurate. It is interesting to note, moreover, that the remaining distance limits are not only satisfied by the ensemble of all trajectory structures but also by each of the subsets of structures discussed above. This may appear surprising because structures representative of these three sets look quite different from each other (see Figure 2a). In fact, this observation points to the general problem of interpreting experimentally measured NOE intensities in terms of a single three-dimen-

Table 1: NOE proton-pair distance [nm] analysis for the *cis* tetramer **1** in $CHCl_3$.[a]

Proton pair	NOE intensity	Model structure	⟨Trajectory⟩	⟨1st cluster⟩	⟨2nd cluster⟩	⟨3rd cluster⟩
N(4)–C6(3)-*pro-R*	w	0.325	0.422	0.432	0.423	0.361
N(4)–C5(4)	m	0.196	0.285	0.292	0.276	0.271
N(4)–C2(3)	w	0.352	0.320	0.316	0.325	0.336
N(4)–C4(4)	w	0.418	0.393	0.363	0.422	0.391
N(4)–C3(2)	w	0.441	0.743	0.732	0.888	0.498
N(3)–C6(3)-*pro-S*	s	0.227	0.262	0.280	0.248	0.241
N(3)–C6(3)-*pro-R*	m	0.285	0.267	0.252	0.281	0.284
N(3)–C6(2)-*pro-R*	m	0.280	0.400	0.355	0.408	0.407
N(3)–C5(3)	m	0.271	0.285	0.287	0.287	0.263
N(3)–C2(2)	w	0.340	0.325	0.332	0.327	0.332
N(3)–C4(3)	w	0.428	0.372	0.430	0.257	0.437
N(3)–C3(1)	w	0.427	0.654	0.507	0.687	0.715
N(2)–C6(2)-*pro-S*	s	0.230	0.253	0.240	0.265	0.257
N(2)–C5(1)	w	0.435	0.430	0.432	0.430	0.428
N(2)–C2(1)	w	0.328	0.321	0.328	0.317	0.319
N(2)–C4(2)	w	0.417	0.395	0.433	0.406	0.370
C4(3)–C6(3)-*pro-R*	m	0.250	0.283	0.249	0.349	0.256
C4(3)–C6(3)-*pro-S*	s	0.232	0.257	0.261	0.246	0.244
C6(3)-*pro-S*–C3(1)	w	0.407	0.830	0.703	0.854	0.868
C6(3)-*pro-S*–C5(3)	s	0.245	0.253	0.236	0.285	0.241

[a] The first column shows the pairs of protons for which experimentally determined NOE data are available. Residue sequence numbers are given in parentheses (see Scheme 1 for reference). The NOE intensities in the second column are only classified as weak (w), medium (m), or strong (s), (Tim Claridge, private communication). The distances in the third column refer to a structure modeled to satisfy all experimental NOE limits. The fourth column reports the distances averaged ($\langle r^{-3}\rangle^{-1/3}$)over the whole ensemble of structures generated in the 100-ns simulation. The following three columns show distances, calculated in analogy from structures in the first, second, and third most populated conformational clusters.

sional structure, as they reflect an averaging over geometries biased ($\langle r^{-3}\rangle^{-1/3}$) towards short proton–proton distances r.[42–44] Clearly this problem is more severe for peptides that show a high degree of conformational flexibility.

Figure 1 shows, as a function of time, the atom-positional root-mean-square deviation (RMSD) of trajectory structures

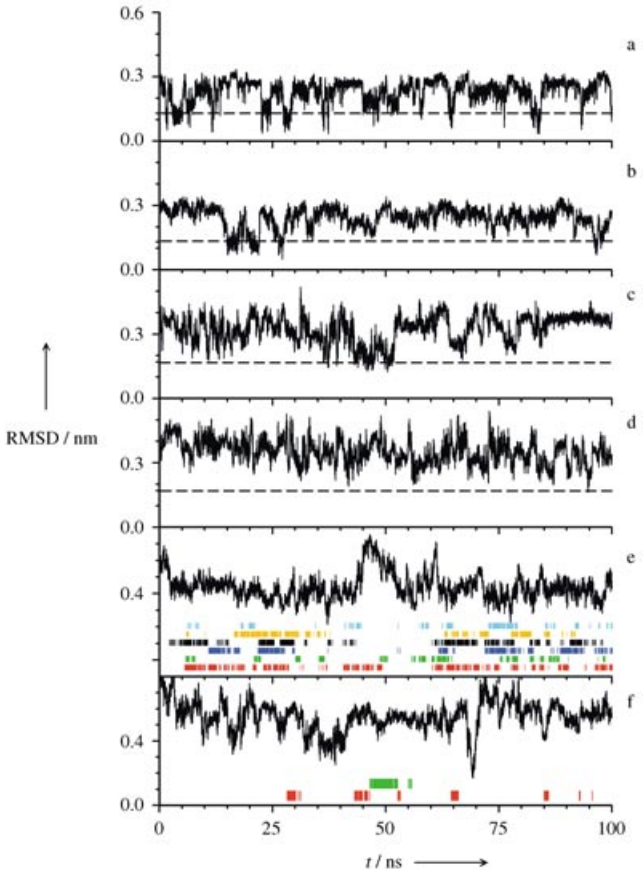

Figure 1. Panels a–e show backbone atom-positional root-mean-square-deviations (RMSD) of trajectory structures from model structures as a function of time. The *cis*-linked tetramer **1** in chloroform and in DMSO (a, b), the *cis* hexamer **2** (c), the *trans* hexamer **4** (d), and the *cis* octamer **3** (e) are compared to hypothetical model structures derived from qualitative NOE data for the *cis* tetramer **1**. The *trans* octamer **5** (f) is compared to a model structure inferred from ref. [31]. Dashed lines indicate the backbone RMSD similarity criterion chosen to define the folded structures. For the *cis* octamer **3** (e), the formation of NH(3)–O(1) (red), NH(4)–O(2) (green), NH(5)–O(3) (blue), NH(6)–O(4) (black), NH(7)–O(5) (orange), and NH(8)–O(6) (cyan) hydrogen bonds is shown as a function of time. For the *trans* octamer **5** (f), we show the formation of hydrogen bonds NH(4)–O(6) (red) and NH(7)–O(3) (green), which characterize, respectively, a 20- and 22-membered hydrogen-bonded ring.

from idealized model structures (see the Experimental Section). We have used all backbone atoms (N, C6, C5, O, C2, C) for this analysis, but excluded the C6, C5, and O atoms of the first residue and the C atom of the last residue (compare with Scheme 1). Single trajectory structures are considered folded if their RMSD from the reference model structure is less than 0.13 (tetramer), 0.17 (hexamers), or 0.28 nm (octamers).

The *cis* tetramer **1** experiences several folding and unfolding events during 100 ns of simulation. With chloroform as solvent, the molecule frequently adopts conformations close to the repeating β-turn right-handed helical model structure (Figure 1 a). This conformation is less often visited when the solvent is DMSO (Figure 1 b). The stronger hydrogen-bonding character of DMSO clearly disfavors formation of intramolecular hydrogen bonds in the peptide. While the hydrogen bonds NH(3)–O(1) and NH(4)–O(2) are, respectively, formed for 11 and 6% of the simulation with chloroform, they occur for only 1 and 3% of the simulation with DMSO as solvent (see the Supporting Information). Analysis of temperature coefficients and chemical shifts leads to similar conclusions.[37]

The folded *cis* hexamer **2** forms four hydrogen bonds of type NH(i)–O($i-2$) with $i = 3$, 4, 5, and 6. Figure 1 c shows the RMSD time series calculated for our MD simulation with chloroform as the solvent. Several folding and unfolding events are observed after about 35 ns. We have not attempted to build a model structure for the *trans* hexamer **4**, as no experimental data have been reported. Figure 1 d shows that it assumes a conformation similar (RMSD < 0.17 nm) to the model of the *cis* isomer only once during the 100 ns of simulation. The *trans* substitution at the THF ring clearly disfavors the formation of the β turn found for the series of *cis*-linked carbopeptoids. Clustering trajectory snapshots into batches of highly similar configurations (see the Experimental Section) generally shows the dominant configurations sampled in an MD simulation. In the case of the *cis* hexamer **3**, we find 11% of all snapshots in the first cluster and a total of 20 significantly (> 1% each) populated clusters, which sums up to 76% of all configurations. These results indicate that the ensemble of *cis*-hexamer configurations is dominated by a fairly small number of different types of structure. The trajectory generated for the *trans* hexamer, however, clusters into significantly more batches. Only 5% of all snapshots are found in the first cluster and a total of 30 significantly populated clusters cover only 62% of all configurations. We conclude that the *trans* hexamer shows a much lower tendency to form any preferred type of secondary structure than the *cis* hexamer. This observation is in line with the experimentally claimed[39] absence of stable secondary structures for short *trans*-linked peptides of the type studied here.

The *cis* octamer **3** folds to a stable structure that shows the same hydrogen-bonding pattern, NH(i)–O($i-2$), as the smaller *cis* oligomers. These hydrogen bonds are observed in our 100-ns-long simulation with chloroform as solvent (Figure 1 e and the Supporting Information). Again, the *trans* octamer **5** shows very different behavior. NH(i)–O($i-2$) hydrogen bonds are not formed at all, a result pointing to the steric constraints imposed by the different stereochemistry. However, other hydrogen bonds, NH(i)–O($i+k$), occur with significant frequency (Figure 1 f and the Supporting Information) to form rings of size 20 ($k = 2$), 22 ($k = -4$), 26 ($k = 3$), 28 ($k = -5$), 32 ($k = 4$), and 38 ($k = 5$). Reflecting their size, these rings are rather flexible and give rise to fairly large RMSD variations (Figure 1 f). A left-handed helix composed of 16-membered rings ($k = -3$) was suggested in experimental NMR studies for a similar *trans* octamer,[40] but this is

observed only once in our simulation (at 69 ns, Figure 1 f). Unfortunately, the experimental paper provides only vague information about the measured NOE values, thereby precluding a direct comparison between NOE and MD data. We note, however, that our analysis of the MD trajectory does not give any indication of long-range contacts of type NH(i)–H5($i-2$), NH(i)–H3($i-3$), H2(i)–H4($i-2$), or H2(i)–H3($i-2$), mentioned in ref. [40] as the calculated values of $\langle r^{-3}\rangle^{-1/3}$ range from 0.7 to 1.2 nm (data not shown).

Figure 2 shows the dominant conformations of the *cis* tetramer **1** and of both the octamers **3** and **5**, together with the corresponding model structures. For the *cis* tetramer, there are 11 clusters populated by at least 1%, which totals 94% of the entire ensemble. The helical model structure falls into the third cluster, whose central member structure shows a similar backbone configuration. For the *cis* and *trans* octamers, we find a larger number of significantly (>1%) populated clusters (27 and 28, respectively), which totals 82 and 87% of the entire ensemble, respectively. The larger diversity of structures reflects the increased conformational flexibility of longer peptide chains. In the case of *cis* octamer **3**, the central member structure of the third cluster displays three examples of the characteristic NH(i)–O($i-2$) hydrogen bonds ($i=3$, 4, and 6) discussed above. One hydrogen bond of this type is also present in the central member structures of the first and second clusters ($i=6$ and 3, respectively).

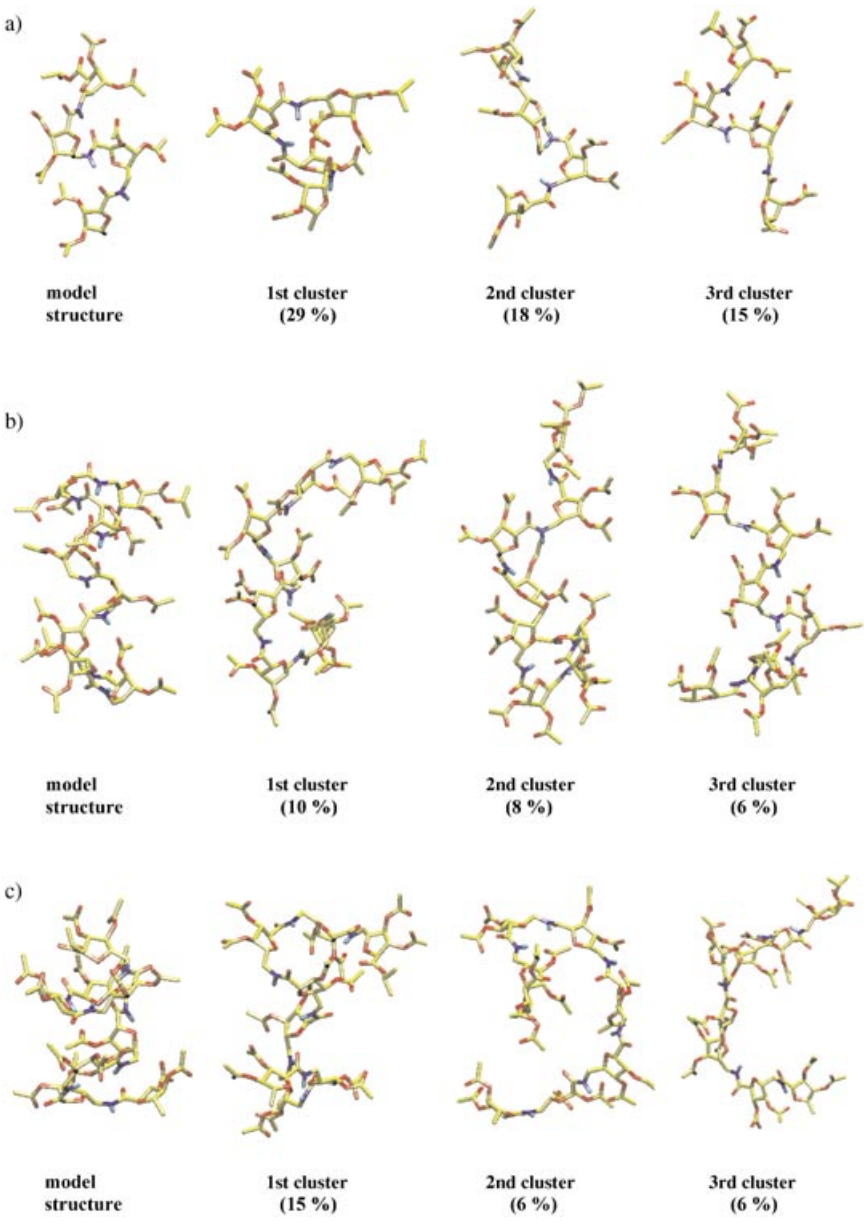

Figure 2. Dominant conformations found for the *cis* tetramer **1** (a), the *cis* octamer **3** (b), and the *trans* octamer **5** (c) in chloroform. Reference model structures are presented to the left, and central member structures of the three most populated clusters are shown on the right. Central member structures are displayed in orientations similar to those chosen for the model structures (superposition of backbone atoms). Populations are given in parentheses.

Carbopeptoids containing THF moieties in their backbone show distinct folding behavior depending on chain length and absolute configuration at the THF–peptide link. The simulations presented herein show good agreement with the, admittedly limited, experimental data available. Sets of NOE data were published only for the tetramer, and they are in good agreement with the simulation. More qualitative conclusions drawn in experimental work are confirmed in the simulations as well. It is important to note that we have not undertaken any attempt to calibrate the force-field parameters specifically for carbopeptoid simulations. Instead we have used a well-calibrated general biomolecular force field which apparently captures the folding behavior of carbopeptoids. Once the agreement with experimental data is established, MD simulations of peptides can be used with some confidence to interpret experimental results in terms of conformational distributions and to explore the various types of secondary structure involved.

Two other major conclusions are apparent from our study: first, it seems misleading to interpret experimentally obtained NOE distance limits in terms of a single dominant structure. In fact, a variety of stable conformations (clusters of structures) is found. Second, the total number of conformations prevailing in the ensemble is still fairly small. This supports a conclusion previously drawn for β-peptides,[15,26] namely that the accessible portion of the unfolded state consists of significantly fewer conformations than expected from simple combinatorial counts of low-energy conformers.

Experimental Section

With the fully extended structures as a starting point, the carbopeptoids **1**–**5** were simulated in (explicit) chloroform and DMSO (only molecule **1**) at 298 K and 1 atm by using the GROMOS96 simulation package[45,46] and the GROMOS biomolecular force field (version 45A3[46,47]). For simulation and analysis details, see the Supporting Information and ref. [48].

The reference (right-handed helical) model structure of the *cis* tetramer **1** was generated by using MD simulations with all available NOE distance limits implemented as additional restraints. This structure is indeed confirmed to satisfy all distance limits (see Table 1). Model structures of the *cis* hexamer **2** and *cis* octamer **3** were constructed in analogy, by assuming the NOE distance limits of the tetramer and augmenting them with the corresponding H–H contacts for the additional residues. This procedure seemed justified, as no experimental data were available to us except for qualitative statements that all *cis* oligomers share analogous NOE patterns. The left-handed helical model structure for the *trans* octamer **5** was built by using qualitative information given in ref. [31].

Received: February 26, 2004 [Z54114]
Published Online: July 19, 2004

Keywords: computer chemistry · conformation analysis · molecular dynamics · peptide folding · tetrahydrofurans

[1] M. Prevost, I. Ortmans, *Proteins Struct. Funct. Genet.* **1997**, *29*, 212 – 227.
[2] X. Daura, B. Jaun, D. Seebach, W. F. van Gunsteren, A. E. Mark, *J. Mol. Biol.* **1998**, *280*, 925 – 932.
[3] Y. Duan, P. A. Kollman, *Science* **1998**, *282*, 740 – 744.
[4] M. Schäfer, C. Bartels, M. Karplus, *J. Mol. Biol.* **1998**, *284*, 835 – 848.
[5] X. Daura, K. Gademann, B. Jaun, D. Seebach, W. F. van Gunsteren, A. E. Mark, *Angew. Chem.* **1999**, *111*, 249 – 253; *Angew. Chem. Int. Ed.* **1999**, *38*, 236 – 240.
[6] M. Takano, T. Yamato, J. Higo, A. Suyama, K. Nagayama, *J. Am. Chem. Soc.* **1999**, *121*, 605 – 612.
[7] A. R. Dinner, T. Lazaridis, M. Karplus, *Proc. Natl. Acad. Sci. USA* **1999**, *96*, 9068 – 9073.
[8] V. S. Pande, D. S. Rokhsar, *Proc. Natl. Acad. Sci. USA* **1999**, *96*, 9062 – 9067.
[9] D. Roccatano, A. Amadei, A. Di Nola, H. J. C. Berendsen, *Protein Sci.* **1999**, *8*, 2130 – 2143.
[10] A. M. J. J. Bonvin, W. F. van Gunsteren, *J. Mol. Biol.* **2000**, *296*, 255 – 268.
[11] P. Ferrara, A. Caflisch, *Proc. Natl. Acad. Sci. USA* **2000**, *97*, 10780 – 10785.
[12] B. Y. Ma, R. Nussinov, *J. Mol. Biol.* **2000**, *296*, 1091 – 1104.
[13] H. W. Wang, S. S. Sung, *J. Am. Chem. Soc.* **2000**, *122*, 1999 – 2009.
[14] X. Daura, K. Gademann, H. Schäfer, B. Jaun, D. Seebach, W. F. van Gunsteren, *J. Am. Chem. Soc.* **2001**, *123*, 2393 – 2404.
[15] W. F. van Gunsteren, R. Bürgi, C. Peter, X. Daura, *Angew. Chem.* **2001**, *113*, 363 – 367; *Angew. Chem. Int. Ed.* **2001**, *40*, 351 – 355.
[16] J. Higo, O. V. Galzitskaya, S. Ono, H. Nakamura, *Chem. Phys. Lett.* **2001**, *337*, 169 – 175.
[17] G. Hummer, A. E. Garcia, S. Garde, *Proteins Struct. Funct. Genet.* **2001**, *42*, 77 – 84.
[18] R. Bürgi, X. Daura, A. E. Mark, M. Bellanda, S. Mammi, E. Peggion, W. F. van Gunsteren, *J. Pept. Res.* **2001**, *57*, 107 – 118.
[19] C. Simmerling, B. Strockbine, A. E. Roitberg, *J. Am. Chem. Soc.* **2002**, *124*, 11258 – 11259.
[20] C. D. Snow, H. Nguyen, V. S. Pande, M. Gruebele, *Nature* **2002**, *420*, 102 – 106.
[21] A. Glättli, X. Daura, D. Seebach, W. F. van Gunsteren, *J. Am. Chem. Soc.* **2002**, *124*, 12972 – 12978.
[22] G. Colombo, D. Roccatano, A. E. Mark, *Proteins Struct. Funct. Genet.* **2002**, *46*, 380 – 392.
[23] H. W. Wu, S. M. Wang, B. R. Brooks, *J. Am. Chem. Soc.* **2002**, *124*, 5282 – 5283.
[24] X. Daura, W. F. van Gunsteren, A. E. Mark, *Proteins Struct. Funct. Genet.* **1999**, *34*, 269 – 280.
[25] H. Schäfer, X. Daura, A. E. Mark, W. F. van Gunsteren, *Proteins Struct. Funct. Genet.* **2001**, *43*, 45 – 56.
[26] X. Daura, A. Glättli, P. Gee, C. Peter, W. F. van Gunsteren, *Adv. Protein Chem.* **2002**, *62*, 341 – 360.
[27] R. Baron, D. Bakowies, W. F. van Gunsteren, X. Daura, *Helv. Chim. Acta* **2002**, *85*, 3872 – 3882.
[28] K. D. Stigers, M. J. Soth, J. S. Nowick, *Curr. Opin. Chem. Biol.* **1999**, *3*, 714 – 723.
[29] M. S. Cubberley, B. L. Iverson, *Curr. Opin. Chem. Biol.* **2001**, *5*, 650 – 653.
[30] D. J. Hill, M. J. Mio, R. B. Prince, T. S. Hughes, J. S. Moore, *Chem. Rev.* **2001**, *101*, 3893 – 4011.
[31] M. D. Smith, G. W. J. Fleet, *J. Pept. Sci.* **1999**, *5*, 425 – 441.
[32] L. Szabo, B. L. Smith, K. D. McReynolds, A. L. Parrill, E. R. Morris, J. Gervay, *J. Org. Chem.* **1998**, *63*, 1074 – 1078.
[33] J. A. Smith, L. G. Pease, *Crit. Rev. Biochem.* **1980**, *8*, 315 – 412.
[34] F. Schweizer, *Angew. Chem.* **2001**, *113*, 240 – 264; *Angew. Chem. Int. Ed.* **2001**, *40*, 230 – 253.
[35] S. A. W. Gruner, E. Locardi, E. Lohof, H. Kessler, *Chem. Rev.* **2002**, *102*, 491 – 514.
[36] T. K. Chakraborty, S. Ghosh, S. Jayaprakash, *Curr. Med. Chem.* **2002**, *9*, 421 – 435.
[37] M. D. Smith, T. D. W. Claridge, G. E. Tranter, M. S. P. Sansom, G. W. J. Fleet, *Chem. Commun.* **1998**, 2041 – 2042.
[38] N. L. Hungerford, T. D. W. Claridge, M. P. Watterson, R. T. Aplin, A. Moreno, G. W. J. Fleet, *J. Chem. Soc. Perkin Trans. 1* **2000**, 3666 – 3679.
[39] M. D. Smith, D. D. Long, A. Martin, D. G. Marquess, T. D. W. Claridge, G. W. J. Fleet, *Tetrahedron Lett.* **1999**, *40*, 2191 – 2194.
[40] T. D. W. Claridge, D. D. Long, N. L. Hungerford, R. T. Aplin, M. D. Smith, D. G. Marquess, G. W. J. Fleet, *Tetrahedron Lett.* **1999**, *40*, 2199 – 2202.
[41] V. P. B. Di Blasio, M. Saviano, A. Lombardi, F. Nastri, C. Pedone, E. Benedetti, M. Crisma, M. Anzolin, C. Toniolo, *J. Am. Chem. Soc.* **1992**, *114*, 6273 – 6278.
[42] X. Daura, I. Antes, W. F. van Gunsteren, W. Thiel, A. E. Mark, *Proteins Struct. Funct. Genet.* **1999**, *36*, 542 – 555.
[43] C. Peter, X. Daura, W. F. van Gunsteren, *J. Biomol. NMR* **2001**, *20*, 297 – 310.
[44] C. Peter, M. Rueping, H. J. Wörner, B. Jaun, D. Seebach, W. F. van Gunsteren, *Chem. Eur. J.* **2003**, *9*, 5838 – 5849.
[45] W. R. P. Scott, P. H. Hünenberger, I. G. Tironi, A. E. Mark, S. R. Billeter, J. Fennen, A. E. Torda, T. Huber, P. Krüger, W. F. van Gunsteren, *J. Phys. Chem. A* **1999**, *103*, 3596 – 3607.
[46] W. F. van Gunsteren, S. R. Billeter, A. A. Eising, P. H. Hünenberger, P. Krüger, A. E. Mark, W. R. P. Scott, I. G. Tironi, *The GROMOS96 Manual and User Guide*, Vdf Hochschulverlag AG, Zürich, **1996**.
[47] L. D. Schuler, X. Daura, W. F. van Gunsteren, *J. Comput. Chem.* **2001**, *22*, 1205 – 1218.
[48] R. Baron, D. Bakowies, W. F. van Gunsteren, *J. Peptide Sci.*, in press.

